Scientific Journals
of the Maritime University of Szczecin

Zeszyty Naukowe
Akademii Morskiej w Szczecinie

2022, 71 (143), 64–71
ISSN 1733-8670 (Printed)
ISSN 2392-0378 (Online)
DOI: 10.17402/519

Received: 30.06.2022
Accepted: 25.07.2022
Published: 30.06.2022

Digital twin of slewing roller bearings operating in wind turbine structures

Marek Krynke

https://orcid.org/0000-0003-4417-1955

Czestochowa University of Technology, Faculty of Management
Department of Production Engineering and Safety
19b Armii Krajowej Ave., 42-218 Czestochowa, Poland
e-mail: marek.krynke@pcz.pl

Keywords: wind turbines, quality, slewing bearings, digital twin, FEM, Industry 4.0

JEL Classification: O30, Q20, Q40

Abstract

A digital twin is a digital replica, a mathematical model of a given object, product, process, system, or service. A digital twin enables the attainment of a significant amount of data and it can be used to gain comprehensive knowledge about a given object, its behaviors, and reactions. The constant ability to monitor the product and its reactions contribute to its improvement and the exclusion of errors, as well as its optimization, which in turn allows for a more perfect product. This article presents a model of a digital twin for the analysis of the operation of a slewing bearing in the structure of a wind turbine. The quality of the bearing is directly related to the quality of the materials from which they were made, the process of thermo-chemical treatment, and the accuracy of all its elements, as well as its proper assembly. The bearings are characterized by very narrow tolerances. Errors in the shape of cylindricity cause distortion of the bearing raceway, stress accumulation, and jamming of rolling parts. This leads to rapid bearing wear as a result. The condition for the approval of bearings for sale is the successful passing of all tests, both geometric and strength. This is to develop quality standards that bearing suppliers must meet. The article presents an analysis of the load distribution that prevail in rotor blade bearings at the limit loads of a wind turbine. The basic types of the most commonly used coronary bearings for wind turbine applications were considered. A methodology for constructing computational models of slewing bearings, using the finite element method, was developed. An original way of simulating rolling parts with rod elements – for rollers and superelements – for the support balls was proposed. A numerical FEM model of a slewing bearing with a wind turbine rotor hub is presented. The calculations accounted for the susceptibility of the bearing rings and hub, as well as the stiffness of the mounting screws. Areas of bearing raceways, where rolling parts achieve the greatest loads, have been identified. Demonstrated by diagrams are the deformations of the rotor hub seats and bearing rings.

Introduction

Wind technology is a particularly demanding application area for rolling bearings. Some of these bearings are very large, subjected to high dynamic loads, and environmental conditions that have a very negative impact on the precision drive components (Szelangiewicz & Żelazny, 2015; Janekova, Fabianova & Rosova, 2016; Idzikowski & Cierlicki, 2021). The drive components of wind turbines (Figure 1) must meet increasingly stringent requirements in terms of durability and strength. Onshore turbines require bearings designed for a service life of 175,000 hours as standard, which is equivalent to 20 years of operation (Zhang et al., 2018). However, in the case of a rapidly growing offshore wind farm market, where high capital expenditures and difficulties in accessing infrastructure are common,

a 25-year bearing service life is expected. This situation is exacerbated by the fact that there are typical damages against which preventive measures should be applied (Staid & Guikema, 2015).

With extreme dynamic loads acting on the wind turbine power unit, the above requirements are a real challenge. In onshore wind turbines, main bearings carry loads of approximately 1 MN. Nevertheless, at sea, due to very high wind speeds, even higher dynamic and static loads act on the rotors and consequently on the entire transmission system (Mattu et al., 2022). Simultaneously, the size and efficiency of systems, both marine and terrestrial, is constantly increasing. A key element of a wind turbine are blades that transfer wind energy in the form of air pressure acting on them to the rotational movement of the rotor. The blades are mounted rotationally in the rotor hub using slewing bearings and, additionally, equipped with servos that allow precise changes to the angle of inclination of the blades (Figure 1). This makes the use of wind energy more efficient and protects the wind farm from wind that is too strong, which can damage or even destroy the turbine (Chou et al., 2013).

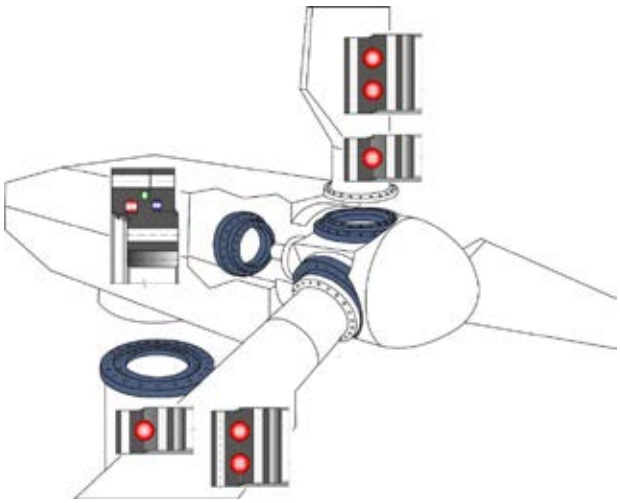

Figure 1. Design solutions for the slewing bearings used in wind turbines

Due to the large dimensions of the blades (from 20 to 100 meters in length) and their weight, which usually exceeds 10 tons, as well as the large moments that act on the blade and adverse environmental impacts (birds, stones, ice, snow, etc.), these elements of the wind turbine structure should be under special supervision. Even minor damage in critical areas of the blade (blade bearing, hub mount, and leading edge) can cause an avalanche increase in damage, until the blade or even the entire turbine is completely destroyed. Thus, wind turbine manufacturers place stringent demands on the load carrying capacity, precision, and durability of the coronary bearings that are used for large wind turbines (Rothe Erde, 2018).

This article presents an analysis of the load distribution that prevail in the bearings fixing the rotor blades at the limit loads of the designed wind turbine. In addition, the maximum radial and axial deformations experienced by the bearing rings and its surfaces, at maximum wind turbine load, are presented by means of graphs.

Slewing bearings – literature review

Slewing bearings are machine components that transfer the entire load from one machine component to another, such as the bodywork to the chassis. Their special features, to which they owe high load capacity with a relatively compact structure and relatively small dimensions, enable them to be used not only in classic machines and devices, such as excavators, and all kinds of cranes and other construction machines and military vehicles, but they are also widely used in wind turbines and many other devices.

An essential feature of these bearings, which distinguishes them from standard bearings, apart from the large diameters, is the design of their bearing rings. These rings are shaped in such a way that they allow you to their attachment with screws directly onto two supporting parts of the device (machine body) – one rotary, the other fixed. Very often, one of the bearing rings is also a toothed wreath, hence the name "slewing bearings". The toothed wreath can be external or internal depending on the location of the cooperating drive gear (Figure 2). The construction of slewing bearings is very diverse. Due to the design features, numerous criteria for division can be distinguished (Smolnicki, 2013), i.e.:

- the form of a toothed wreath – external and internal;
- raceway construction – soft, hard, monolithic, and wire;
- type of rolling elements – ball, roller, and ball-roller;
- number of raceways in a row – single-row and multi-row;
- number of treadmills cooperating with the rolling element – i.e., two-raceway, four-raceway.

Due to the specific nature of the operation of slewing bearings – slow rotational or oscillating movements – these bearings are mainly calculated for the static load carrying capacity conditioned

by the maximum allowable pressure in the contact zone of the most loaded rolling element (Krynke & Mielczarek, 2016). This is the basic criterion for the selection of coronary bearings for most applications. Gradual wear of the treadmill (most often by pitting), or occasional pitting chips, do not affect the smoothness and accuracy of movement for a significant amount of time (Vicen et al., 2020).

The load carrying capacity of the slewing bearings usually limits the maximum value of external loads of the designed device, and its correct determination is an important part of the calculation of the working machine. Slewing bearings are usually selected for extremely limits, that is, so that their work is at their limit of strength. This requires careful and accurate calculations of their performance parameters, of which the static load capacity is still the most important, which is increasingly supplemented with additional criteria from assembly and durability to determination of resistance to movement (Aguirrebeitia et al., 2012; Kania, Krynke & Mazanek, 2012). It should be borne in mind that in many devices damage or destruction of the coronary bed can cause catastrophic accidents. In addition, it requires the machine to be removed from service for a long time and results in high repair costs (Jin et al., 2021; Nedeliaková, Hranický & Valla, 2022). Therefore, slewing roller bearings in the vast majority of machines can be counted among their most responsible components. There are also high demands on the load carrying capacity and reliability of these bearings. For this reason, rolling bearings have been the subject of intensive research for many years meaning that, over time, bearing technology has developed into a separate branch of knowledge.

In the technical documentation of slewing bearings, the static load carrying capacity is presented in the form of the so-called static load carrying capacity characteristics (Rothe Erde, 2018). It contains the relation of the interdependence of the transmitted subversive moment M with the axial force Q for the assumed value of the radial force H (Figure 2). These characteristics regulate the range of permissible loads that a bearing is able to safely carry assuming a service life specified by the manufacturer.

The load capacity of a slewing bearing depends not only on the strength of the raceway, but also on the strength of the bolts that fix the bearing rings to the supporting structures (Krynke & Ulewicz, 2019). Screws largely affect the stiffness of the support system: bearing rings and supporting components. Therefore, in the design solution of any slewing bearing, it is very important to choose the right

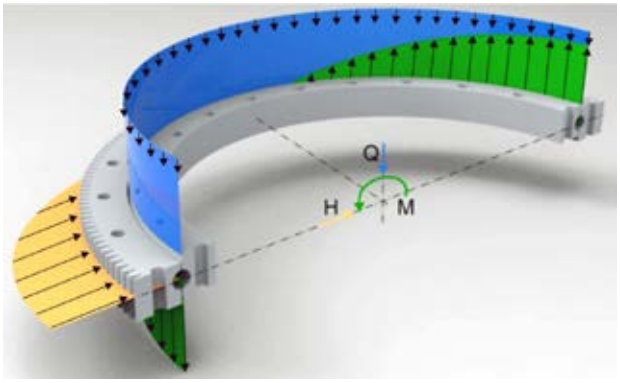

Figure 2. Ability of the slewing bearing to carry three load components *M*, *Q*, and *H*

number, diameter, and strength class of fixing screws (Krynke, 2016).

Classical methods of calculation of slewing bearings, based on the assumption of rigid rings, quickly allow a determination of the load distribution and the angles of action of rolling parts located around the raceway circumference and, thus, determine the most critical sector of the bearing (Gibczyńska & Pytko, 1999). However, in slewing bearings placed on supporting structures, whose seats are characterized by varying stiffness around the perimeter, the load on some rolling parts may exceed even several times the load calculated with the assumption of rigid rings (Smolnicki, 2013). Hence, there is a need to have a calculation model that enable an account of not only the stiffness of the bearing rings, but also the susceptibility of the machine supporting structures and the susceptibility of fastening.

The selection of slewing roller bearings is most often performed on the basis of static load carrying capacity diagrams called characteristics (Mazanek, 2005). The static load rating characteristics result from the distribution of the load per the individual rolling elements along the perimeter of the bearing raceway.

Methodology

As part of the numerical analysis, concerning the determination of the loads that prevail in the bearings of the rotor blades of a wind turbine, a three-blade wind farm with a horizontal axis of rotation with a control system based on changing the angle of the blades was considered. A catalogue single row slewing ball bearing with a four-point contact (Figure 3) was used for the calculations, its parameter are as follows:

- rolling diameter d_t = 2000 mm,
- diameter of balls d = 50 mm,

- number of balls $z = 94$,
- coefficient of adhesion of the ball to the raceway $k_p = 0.96$,
- nominal operating angle $\alpha_0 = 45°$,
- raceway hardness – 54 HRC,
- number of mounting screws – 40 screws M30-10.9 in each ring.

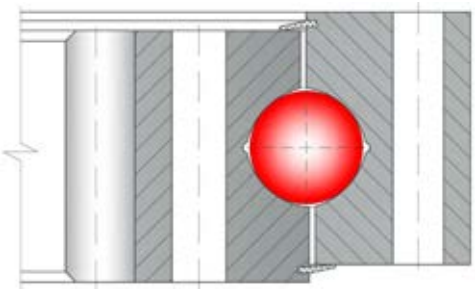

Figure 3. Single row slewing ball bearing with four-point contact

In addition, it was assumed that:

- the rolling radii, on which the rolling parts roll in the carrying and support rows, are the same;
- raceway surfaces and rolling parts have perfect shapes, and all rolling parts have the same diameter;
- the materials of the rings and rolling parts are homogeneous and isotropic.

When calculating the load carrying capacity of slewing roller bearings, two issues are directly relevant related to the rolling parts:

- determination of the maximum force that can be loaded onto the rolling element and the associated maximum deformation of the rolling part and raceway;
- determination of the nature of the relationship between the load of the ball and its deformation, and the actual mutual approximation of the bearing raceway.

It was assumed that the limit load of the ball is the force causing the relative plastic deformation $\delta_{\text{pl dop}}$, so that (Mazanek, 2005):

$$\delta_{\text{pl dop}} / d = 2 \cdot 10^{-4} \tag{1}$$

The maximum force that can be loaded on the ball-raceway system was calculated from the relationship (Kania, 2005):

$$F_{\text{dop}} = 9.9626 \cdot 10^7 f_H d^2 / c_p^2 \text{ [N]} \tag{2}$$

where d [mm] represent the ball diameter, c_p [MPa$^{2/3}$] denotes the pressure constant in the point contact zone, and f_H is the corrective hardness coefficient (Eschmann, Hasbergen & Weigand, 1978).

The deformation of the ball and, thus, the approximation of the bearing raceway determines the relationship:

$$\eta = c \cdot F^w \tag{3}$$

where c represents the constant depending on the geometry and materials of the elements in contact and w denotes the power exponent; in these calculations it was assumed that $c = 0.000122$ and $w = 2/3$ (Kania, 2005).

Determining the design loads of a wind turbine was established using previously used parameters (Troen & Lundtang Petersen, 1989; Czapla, Jureczko & Pawlak, 2010), such as:

- blade length equals 45 m,
- global variable of the speed of rotation $\lambda = 6$,
- rotor of the wind turbine is at a height 80 m,
- average wind speed is 9.7 m/s.

Local coordinate systems (Figure 4) based on PN-IEC 61400-1 (DNV, 2009) were used to determine the load of the bearings with which the blades are mounted in rotation in the rotor hub. The x-axis direction is perpendicular to the main shaft axis in the plane of rotation of the blade bearing, while the y-axis direction coincides with the main shaft axis in a plane perpendicular to the bearing axis and the z-axis aligns with the blade bearing axis.

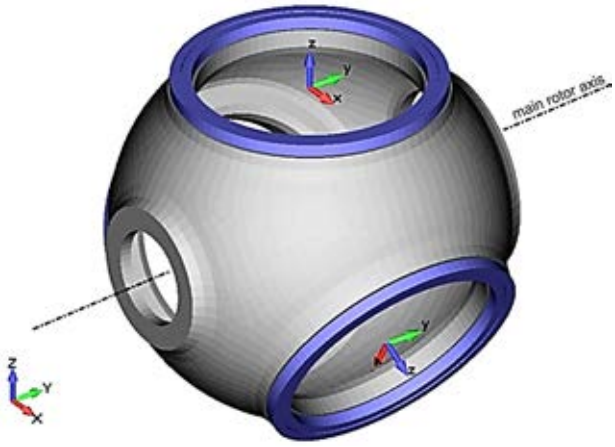

Figure 4. Directions of the local coordinate systems in the numerical model of the rotor hub body alongside the blade bearings

When performing a numerical analysis of the internal load distribution in the rotor blade bearings, a load consisting of forces (F_x, F_y, and F_z) and moments (M_x and M_y) was taken into account. A load case characterized by the maximum value of torque M_y was assumed. The values of forces and moments in local coordinate systems for blades 1, 2, and 3 for the adopted design load variant are presented in

Table 1 (Czapla, Jureczko & Pawlak, 2009). Forces were applied to the individual blade bearings in accordance with the requirement that, for numerical calculations taking into account the deformation of the rotor hub, the load should be applied to all bearings at the same time.

Table 1. Values of loads of individual bearings transferring loads from the blades to the rotor hub of the wind turbine

	Blade bearing 1	Blade bearing 2	Blade bearing 3
F_x [kN]	–70	20	40
F_y [kN]	300	–350	150
F_z [kN]	–65	80	–15
M_x [kNm]	–7500	5700	1700
M_y [kNm]	2400	–200	–370

The numerical model of the hub assembly and blade bearings was made in the ADINA program (Figure 5). 8-nodal solid elements were used to discretize the bearing rings, similar to the rotor hub and bearing housing rings on the blade mounting side. A superelement (Smolnicki, 2002) was used to model the balls, in which non-linear rod elements were used to ensure the transfer of only tensile forces and appropriate stress-deformation characteristics. The surrogate characteristics have been corrected by taking into account the finite element susceptibility in the raceway model, with a view of ensuring that the stiffness of the superelement corresponds to the relationship between the load on the ball and its deformation, and the actual mutual approximation of the bearing raceway (Kania, 2005).

The bearing with hub and blade seats is fixed by means of pre-tensioned bolted connections. The bolts that fasten the rings of slewing bearings to support structures are an important part of the entire swing mechanism. They greatly affect the stiffness of the bearing rings, at the same time the strength of the screws often determines the load capacity of the entire working system. For their modeling, special beam elements were used, which can be attributed to the assumed preload in the form of force (Krynke & Ulewicz, 2019). Figure 5 shows the numerical model used in the calculations. Appropriate boundary conditions that result from attaching the hub to the main axis of the rotor were introduced to the model. Suitable contact surfaces between the bearing rings and the seats of the hub and the rotor blade have been defined. At the junction of the joined elements, a coefficient of friction of 0.15 is assumed.

The bearing load is applied to its outer ring by means of additional constrain bonds superimposed

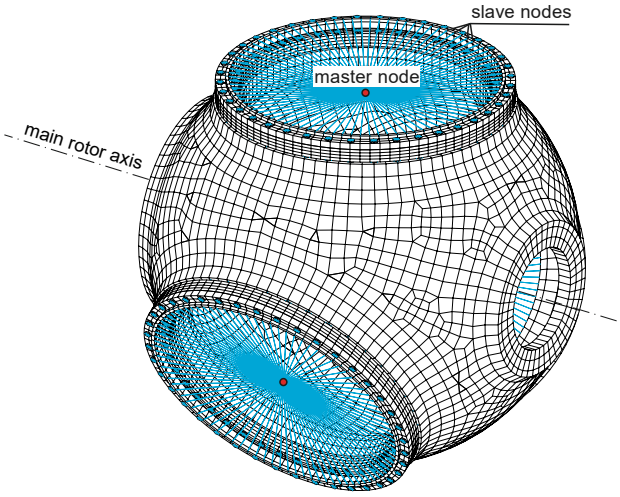

Figure 5. Numerical model of selected components of a wind power plant

on the mesh nodes of the upper surface of the blade girder; this is shown in Figure 5. Constraints rigidly connect the nodes of the upper surface of the shovel ring (slavenodes) to the masternode located in the bearing axis. The external load of the bearing in the form of concentrated forces and focused moments is applied to the masternode. Slave nodes experience the same displacements and rotations as the master node and retain their coplanarity when the load is applied.

Analysis of obtained results from numerical calculations

Figure 6 shows the internal load distributions in the bearings for the three rotor blades. The graphs use the Cartesian coordinate system, defining the abscissa axis as the angle of distribution of individual rolling parts, while the ordinate axis represents the so-called, e.g., specific load of the ball (Smolnicki, 2002). The diagrams show that both the row of capacity and support balls take a similar share in transferring loads from the blade to the rotor hub. It follows that the predominant bearing load on the rotor blade bearings of wind turbines is the tilting torque.

From the distribution of loads carried by the rolling elements shown in Figure 6, it is clear that the most heavily loaded is in the bearing of blade 1. The values of the loads carried by some rolling elements exceed the limit values. It should also be noted that a clearance-free bearing was used for analysis. If there is a clearance that increases over the life of the bearing, the number of rolling elements involved in load transfer is reduced (Kania, Pytlarz & Śpiewak, 2018). This changes the distribution of

the internal load, resulting in an additional increase in the loads on the rolling elements that relate to transferring loads from one bearing ring to another.

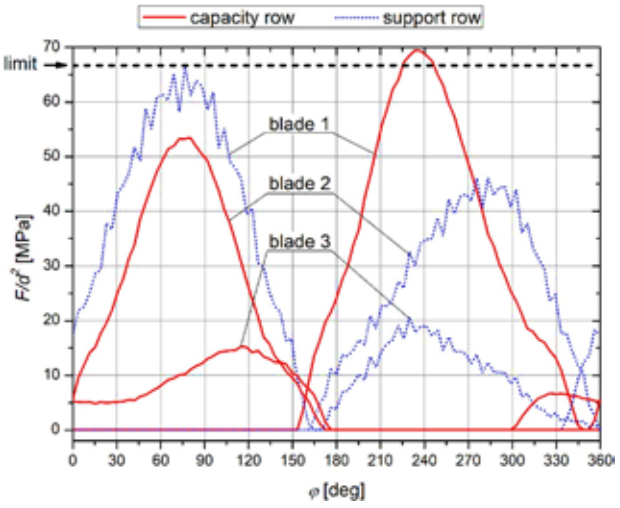

Figure 6. Internal load distribution in the bearings of individual blades, with the wind turbine rotor loaded with maximum design forces

From the presented example, it can also be concluded that the single row bearing used is too heavily loaded. Hence, for the wind turbine used in the analysis on the rotor blade bearings, it is advisable to use double slewing bearings (Figure 1).

Figure 7 shows the deformed plane of the hub seat and the bearing ring represented by a cloud of points, defined by finite element nodes located on these surfaces. On this graph, a plane is plotted approximating the location of these points. By calculating the distances of these points from the approximating plane, the maximum deviation from the flatness (deplanation) of these surfaces was determined. The individual values of these deviations, for blade 1 (the most loaded), are shown in the diagram of Figure 8. The maximum values of these deviations are approximately 0.3 mm.

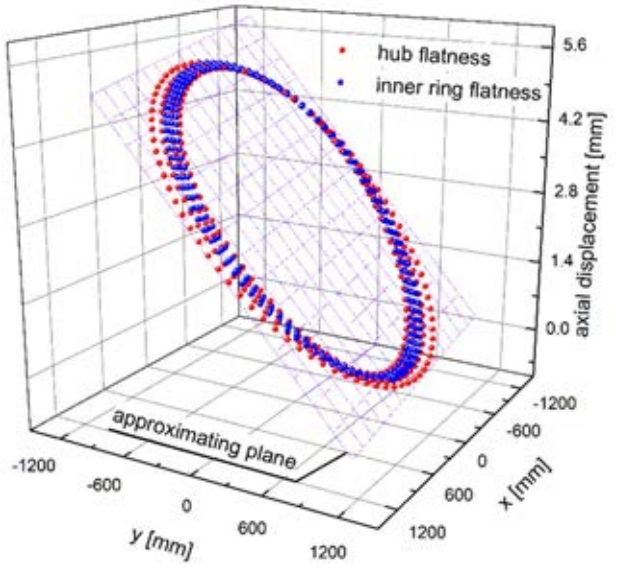

Figure 7. Deformation of the hub seat, and the inner ring of the bearing, for blade 1

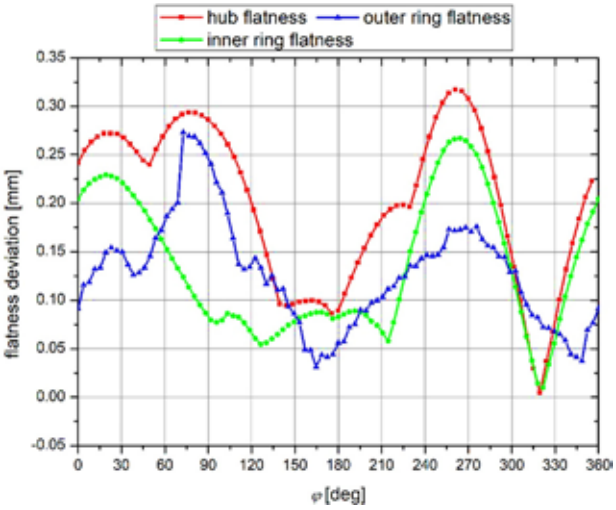

Figure 8. Maximum deviation from flatness (deplanation) of the hub seat and bearing ring mounting surface for blade 1

It is noteworthy that the global manufacturer of slewing bearings, Rothe Erde, allows for this bearing deplanation of the seats of supporting components at the level of 0.3 mm (Rothe Erde, 2018). Taking into account the above results, as well as the distribution of loads in the rotor bearings, the course of which is even (without excessive accumulations), it can be concluded that the rotor hub in terms of operation of slewing bearings is correctly designed.

As a result of large and complex loads, the slewing bearing rings also suffer radial deformation. Figure 9 shows the distribution of these deformations around the bearing circumference for blade no. 1. The maximum values of these displacements are approximately 3 mm, with this deviation being related to the significant rolling diameter of the bearing, which in this case is 2 m.

Figure 10 shows the forces acting on the individual screws that attach the blades to the rotor hub. From the presented results, it can be concluded that the screws that carry the highest loads are forced to approximately 85% of their tensile strength. In this case, however, keep in mind that these screws are loaded eccentrically, which means that they also contain bending moments in addition to tensile forces (Krynke, 2016). Therefore, in the case of the analysis of bolted connections of this type, it is advisable to conduct further analyzes taking into account these factors.

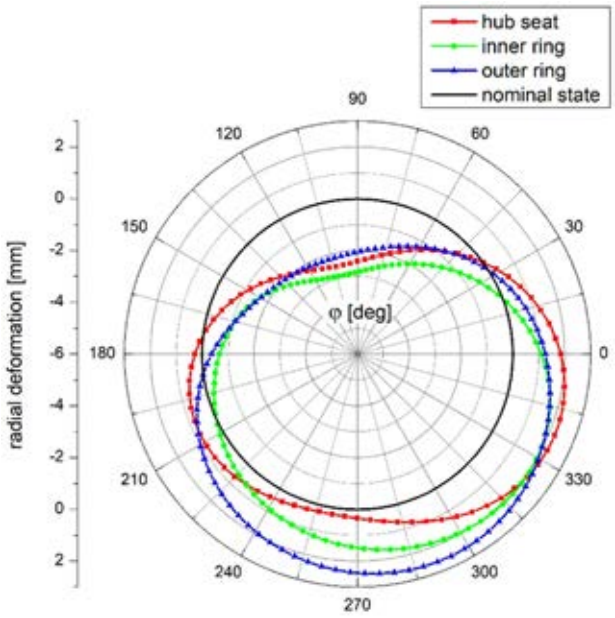

Figure 9. Radial deformations of the hub seat and the mounting surface of the blade bearing rings 1

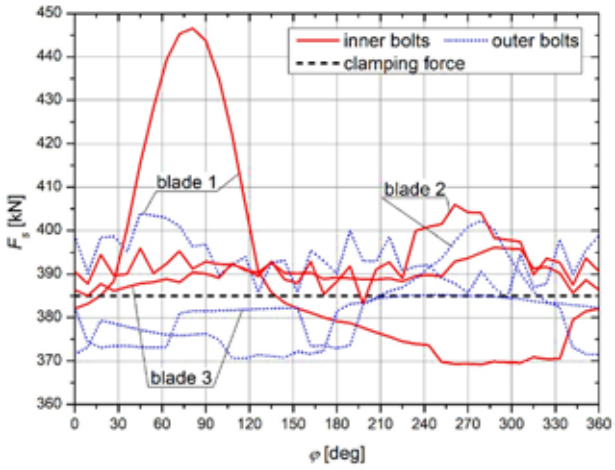

Figure 10. Loading on the screws fixing the inner ring of the bearing to the rotor hub, and the screws fixing the blades to the outer ring of the slewing bearings, with the wind turbine rotor loaded with maximum design forces

Figure 11 shows a map of reduced stresses according to the Huber's hypothesis. The maximum stress of the hub is about 165 MPa, while the tensile strength of the hub material (spheroidal graphite cast iron EN-GJS-400-18U-LT) is R_m = 370 MPa. Hence, the lowest safety factor is 2.2. The average values of the general safety factor for malleable cast iron for variable loads are 3.5–4 (Czapla, Jureczko & Pawlak, 2009). In the case of wind turbines, in addition to the material factor, one should also take into account the factor that depends on the adopted variant of the power plant loads and the factor determining the consequences of failure (DNV, 2009).

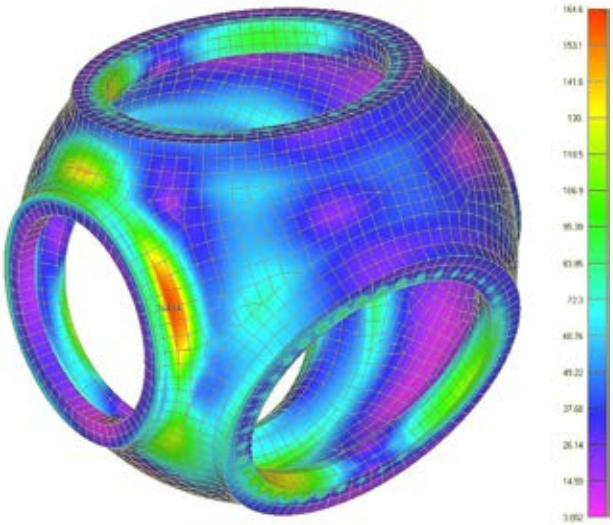

Figure 11. Huber-Mises stress distribution in the rotor hub of the wind turbine, with maximum design forces load

Therefore, it can be concluded that the safety factor for the rotor hub is insufficient for the maximum loads that occur in extreme cases of wind turbine operation. However, for definitive conclusions to be drawn, a more detailed analysis of the hub strength should be performed. This article has focused more on the load capacity of the hub bearings.

Conclusions

The presented analysis proved the suitability of using numerical methods in practical calculations. It allowed an accurate determination of the distribution of forces transmitted by individual rolling elements of the bearing. Such modeling enables a quick verification of all the structural or technological changes introduced both to the geometry of the bearing and to the structures of its installation.

The calculations carried out on selected parts of the wind turbine show that the rotor hub is characterized by an insufficient value of the safety factor for the maximum loads that occur in extreme cases of wind turbine operation. Taking into account the range of deformations experienced by the rotor hub seats, as well as the distribution of loads in the rotor bearings, the course of which is uniform (without excessive accumulations), it can be determined that the rotor hub in terms of operation of slewing bearings is correctly designed.

From the example presented in this article, it can also be concluded that the single row ball bearing with a four-point contact used is too heavily loaded. Hence, for the wind turbine analyzed in this study for the rotor blade bearings, it would be advisable to use double slewing bearings.

References

1. Aguirrebeitia, J., Abasolo, M., Avilés, R. & Fernández de Bustos, I. (2012) General static load-carrying capacity for the design and selection of four contact point slewing bearings: Finite element calculations and theoretical model validation. *Finite Elements in Analysis and Design* 55, pp. 23–30, doi: 10.1016/j.finel.2012.02.002.
2. Chou, J.-S., Chiu, C.-K., Huang, I.-K. & Chi, K.-N. (2013) Failure analysis of wind turbine blade under critical wind loads. *Engineering Failure Analysis* 27, pp. 99–118, doi: 10.1016/j.engfailanal.2012.08.002.
3. Czapla, T., Jureczko, M. & Pawlak, M. (2009) Wyznaczanie współczynnika bezpieczeństwa wybranych części elektrowni wiatrowej. *Acta Mechanica et Automatica* 3(3), pp. 16–22.
4. Czapla, T., Jureczko, M. & Pawlak, M. (2010) The application of modern computer aided engineering systems in design and strength simulations of the chosen components of the wind turbine. *Górnictwo Odkrywkowe* 51(4), pp. 245–251.
5. DNV (2009) *Guidelines for Design of Wind Turbines*. 2nd edition. Copenhagen: DNV.
6. Eschmann, P., Hasbergen, L. & Weigand, K. (1978) *Die Wälzlagerpraxis.* München: Oldenburg Verlag.
7. Gibczyńska, T. & Pytko, S. (1999) Łożyska toczne wieńcowe. Kraków: Uczelniane Wydawnictwa Naukowo-Dydaktyczne AGH.
8. Idzikowski, A. & Cierlicki, T. (2021) Economy and energy analysis in the operation of renewable energy installations – a case study. *Production Engineering Archives* 27(2), pp. 90–99, doi: 10.30657/pea.2021.27.11.
9. Janekova, J., Fabianova, J. & Rosova, A. (2016) Environmental and economic aspects in decision making of the investment project "wind park". *Polish Journal of Management Studies* 13(1), pp. 90–100, doi: 10.17512/pjms.2016.13.1.09.
10. Jin, X., Chen, Y., Wang, L., Han, H. & Chen, P. (2021) Failure prediction, monitoring and diagnosis methods for slewing bearings of large-scale wind turbine: A review. *Measurement* 172, 108855, doi: 10.1016/j.measurement.2020.108855.
11. Kania, L. (2005) *Analiza obciążenia wewnętrznego w łożyskach tocznych wieńcowych w aspekcie ich nośności statycznej.* Częstochowa: Wydawnictwa Politechniki Częstochowskiej.
12. Kania, L., Krynke, M. & Mazanek, E. (2012) A catalogue capacity of slewing bearings. *Mechanism and Machine Theory* 58, pp. 29–45, doi: 10.1016/j.mechmachtheory.2012.07.012.
13. Kania, L., Pytlarz, R. & Śpiewak, S. (2018) Modification of the raceway profile of a single-row ball slewing bearing. *Mechanism and Machine Theory* 128, pp. 1–15, doi: 10.1016/j.mechmachtheory.2018.05.009.
14. Krynke, M. & Mielczarek, K. (2016) Analysis of causes and effects errors in calculation of rolling slewing bearings capacity. *Production Engineering Archives* 12, pp. 38–41, doi: 10.30657/pea.2016.12.09.
15. Krynke, M. & Ulewicz, R. (2019) Analysis of the influence of slewing bearing mounting on their static load capacity. *Transportation Research Procedia* 40, pp. 745–750, doi: 10.1016/j.trpro.2019.07.105.
16. Krynke, M. (2016) Numerical analysis of bolts loading in slewing bearing. *Czasopismo Techniczne. Mechanika* R.113 (z. 4-M (14)), doi: 10.4467/2353737XCT.16.237.5986.
17. Mattu, K.L., Bloomfield, H.C., Thomas, S., Martínez-Alvarado, O. & Rodríguez-Hernández, O. (2022) The impact of tropical cyclones on potential offshore wind farms. *Energy for Sustainable Development* 68, pp. 29–39, doi: 10.1016/j.esd.2022.02.005.
18. Mazanek, E. (2005) *Zagadnienia konstrukcyjne i wytrzymałościowe w wielkogabarytowych łożyskach tocznych wieńcowych*. Częstochowa: Wydawnictwa Politechniki Częstochowskiej.
19. Nedeliaková, E., Hranický, M.P. & Valla, M. (2022) Risk identification methodology regarding the safety and quality of railway services. *Production Engineering Archives* 28(1), pp. 21–29, doi: 10.30657/pea.2022.28.03.
20. Rothe Erde (2018) *Slewing Bearings – Customer-specific solutions for individual requirements*.
21. Smolnicki, T. (2002) *Fizykalne aspekty koherencji wielkogabarytowych łożysk tocznych i odkształcalnych konstrukcji wsporczych.* Wrocław: Oficyna Wydawnicza Politechniki Wrocławskiej.
22. Smolnicki, T. (2013) *Wielkogabarytowe toczne węzły obrotowe, zagadnienia globalne i lokalne*. Wrocław: Oficyna Wydawnicza Politechniki Wrocławskiej.
23. Staid, A. & Guikema, S.D. (2015) Risk analysis for U.S. offshore wind farms: the need for an integrated approach. *Risk Analysis: An Official Publication of the Society for Risk Analysis* 35(4), pp. 587–593, doi: 10.1111/risa.12324.
24. Szelangiewicz, T. & Żelazny, K. (2015) Sea wind farms. *Sea Wind Farms* (41), pp. 35–40, doi: 10.17402/005.
25. Troen, I. & Lundtang Petersen, E. (1989) *European Wind Atlas*. Denmark.
26. Vicen, M., Bokůvka, O., Nikolić, R. & Bronček, J. (2020) Tribological behavior of low-alloyed steel after nitriding. *Production Engineering Archives* 26(3), pp. 78–83, doi: 10.30657/pea.2020.26.16.
27. Zhang, X., Liu, J., Han, Y. & Du, X.-L. (2018) A framework for evaluating the bearing capacity of offshore wind power foundation under complex loadings. *Applied Ocean Research* 80, pp. 66–78, doi: 10.1016/j.apor.2018.08.019.

Cite as: Krynke, M. (2022) Digital twin of slewing roller bearings operating in wind turbine structures. *Scientific Journals of the Maritime University of Szczecin, Zeszyty Naukowe Akademii Morskiej w Szczecinie* 71 (143), 64–71.